➢ ***ORAL PRESENTATION***

Effect of Cathode Shape and Anodization Time on The Formation of TiO_2 Nanotubes on Ti6Al4V-ELI Alloy

Elif Çitgez[1] (*ORCID: https://orcid.org/0009-0007-8415-5083*), Ferda Mindivan[2*] (*ORCID: https://orcid.org/0000-0002-6046-2456*), Harun Mindivan[1](*ORCID: https://orcid.org/0000-0003-3948-253X*)

[1]Bilecik Şeyh Edebali University, Engineering Faculty, Mechanical Engineering Department, Bilecik, Turkey
[*2]Bilecik Şeyh Edebali University, Engineering Faculty, Bioengineering Department, Bilecik, Turkey

*Corresponding author e-mail: ferda.mindivan@bilecik.edu.tr

Abstract
The aim of this work was to determine the effect of cathode type and anodization time on the formation of a compact and nanotubular oxide layer on the Ti6Al4V ELI alloy. The results showed that using a square graphite cathode and an anodic oxidation time of 60 minutes were the most suitable parameters for forming a homogeneous nanotubular layer on the Ti6Al4V ELI alloy. Under these conditions, the nanotube diameter of the SGC-60-coded sample was 73.02 nm, the contact angle was 99.27°, and the surface roughness (Ra) was determined to be 0.11 µm. This study suggests that when an organic electrolyte solution containing ammonium fluoride and ethylene glycol is used in the anodic oxidation process, a square graphite cathode and 60 minutes of anodic oxidation time are sufficient to form a regular nanotube structure with uniform tube distribution.

Keywords: Ti6Al4V-ELI alloy, Anodic oxidation conditions, Nanotube form.

INTRODUCTION

Titanium and its alloys have been used as biomaterials for dental implants and orthopedic prostheses because of their excellent strength-to-weight ratio, adequate corrosion resistance, bio-inertness, low cytotoxicity, and favorable biocompatibility (Matykina et al., 2011; Ansari et al., 2020). Ti-6Al-4V ELI alloy is the most frequently used titanium-based biomaterial (Kiel et al., 2012). Ti6Al4V ELI contains aluminum and vanadium as stabilizing elements, with aluminum stabilizing the alpha phase and vanadium stabilizing the beta phase. These elements enhance the corrosion and mechanical properties of the alloy. However, under specific tribocorrosion conditions, aluminum and vanadium can be released as ions from the material, potentially leading to harmful effects (Gabor et al., 2020). The native oxide layer, typically 1–5 nm thick, naturally forms on the surface of titanium alloys and helps prevent ion release. This oxide layer plays a crucial role in the high biocompatibility of titanium alloys by acting as a protective barrier that minimizes the potential for harmful ion leakage into the body (Lario et al., 2019). An electrochemical technique known as anodization or anodic oxidation is a surface treatment technique applied to titanium alloys that generates regular nano topographical features, such as nanotubes. These nanotubes are contributed significantly to preventing ion release, enhancing properties like biocompatibility and osseointegration (Yavari et al., 2015; Wang et al., 2014). With recent developments in the creation of nanostructured surfaces, it has been successfully applied as a surface treatment for orthopedic implants throughout the previous few decades. In particular, modifying the anodic conditions makes it simple to build and control self-organized nanotubular oxide structures (Wang et al., 2014). Numerous studies in the literature investigate the impact of anodic oxidation conditions on the nanotube structures produced on Ti alloys (Jáquez-Muñoz et al., 2024; Gaona-Tiburcio et al.,2024; Andoko et al. 2024; Jáquez-Muñoz et al., 2023; Kapusta-Kołodziej et al., 2017; Jarosz et al., 2014; Kapusta-Kołodziej et al., 2014; Kim et al., 2013). In this study, the effect of cathode shape and anodization time used in the anodic oxidation process to form nanotubes on Ti6Al4V ELI alloy was examined.

MATERIALS and METHODS

In this study, a purchased 1 m Ti6Al4V ELI rod was cut into 20 mm diameter sections, grounded, and polished (Figure 1(a)). It was then prepared for anodization by ultrasonic cleaning with ethanol for 5 minutes, followed by 5 minutes of cleaning with deionised water. Ti6Al4V-ELI was used as the working electrode (anode) and square, cylindrical graphite cathode as the cathode (Figure 1(b)). Images of square and cylindrical graphite cathodes used during the anodic oxidation process are given in Figure 1 (c) and (d). The anodizing parameters and the codes of the samples produced with different parameters are shown in Table 1. Surface analysis of samples after anodic oxidation treatment were examined by field emission scanning electron microscopy (FE-SEM (Supra 40VP, Zeiss)). The contact angles of the samples were measured with the Fytronix 9000 Contact Angle Analyzer device. The surface roughness values of the samples were measured with the Mitutoyo Surtest SJ-400 profilometer.

Table 1. The anodizing parameters and samples codes.

Samples	Graphite Cathode	Anodization Time (min.)	Voltage (V)	Organic Electrolyte Solution
SGC-30	Square	30	60	%0.5 N_4F %5.0 H_2O Balanced Ethylene Glycol
SGC-60	Square	60	60	
CGC-30	Cylindrical	30	60	
CGC-60	Cylindrical	60	60	

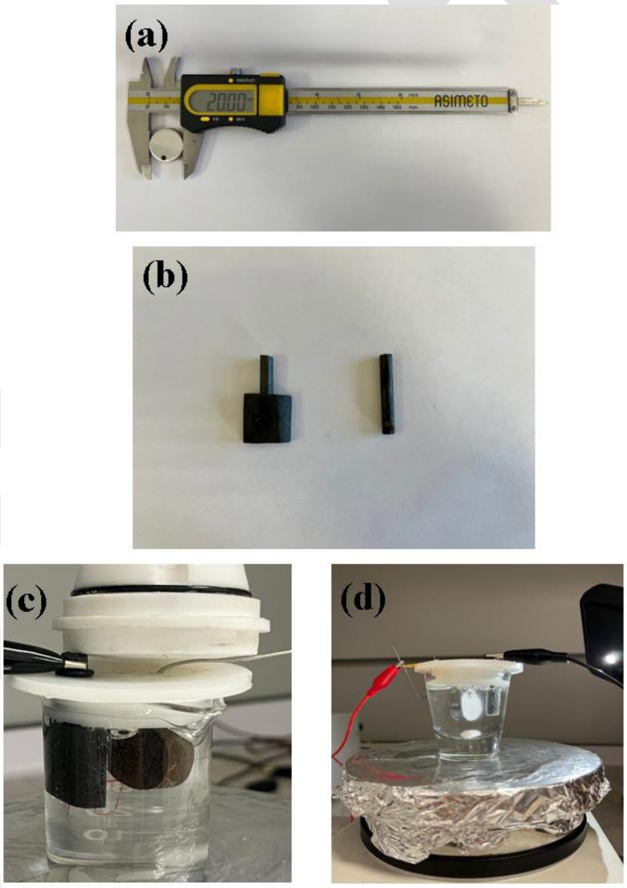

Figure 1.(a) Ti6Al4V ELI alloy, (b) Square and cylindrical graphite cathode, (c) Anodic oxidation with square graphite cathode and (d) Anodic oxidation with cylindrical graphite cathode.

RESULTS and DISCUSSION

Figure 2 (a-d) shows the nanotubular layers obtained from FE-SEM images after the anodic oxidation process. The various combinations of anodic oxidation parameters led to significantly different nanotube sizes and structures on the surface of samples. No regular nanotube structure was observed on the surface of the SGC-30, CGC-30 and CGC-60 samples (Figure 2(a), (b), and (d)). A regular nanotube structure was only present in the SGC-60 sample where a square graphite cathode was used, and oxidation was carried out for 60 minutes (Figure 2(c)). The regular nanotube structure seen in Figure 2(c) is similar to the nanotube morphology formed after anodic oxidation on Ti6Al4V-ELI alloy in the literature (Lario et al., 2019). As shown in Figure 2(b), the nanotube orientations are distinct in the oxidation process performed with a cylindrical cathode for 30 minutes. However, Figure 2(d) clearly demonstrates that while the orientations change in the oxidation process conducted under the same conditions for 60 minutes, a uniform tube distribution is not achieved across the entire surface. Figure 3(a-b) shows the nanotube sizes and angles obtained after the anodic oxidation process with square cathode at different times. As seen in Figure 3 (a), the average nanotube diameter of the SGC-30 coded sample was 55.55 nm and the average angle was 328.48°. As seen in Fig. 3(b), the average nanotube diameter of the SGC-60 coded sample was 73.02 nm and the average angle was 285.27°. It was observed that as the anodic oxidation time increased, the nanotube diameters enlarged, while the angle decreased. In previous anodic oxidation studies, it has been reported multiple times that the nanotube diameter increases with anodic oxidation time (Mazierski et al., 2016; Gong et al., 2001).

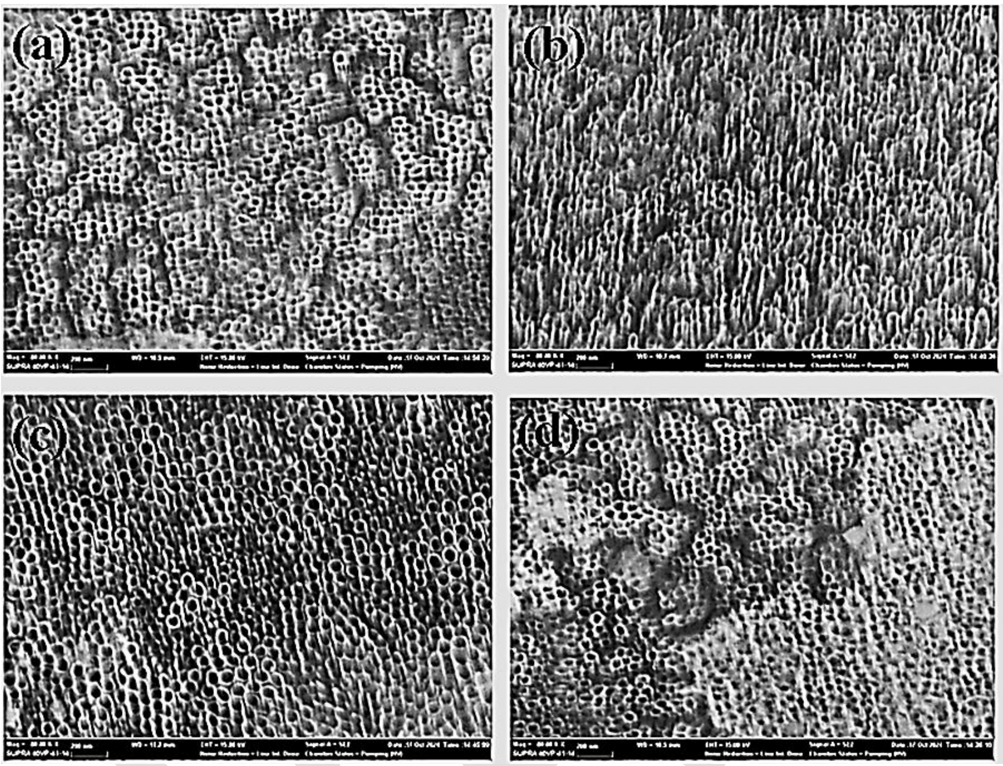

(a) (b)

Figure 2. FE-SEM images of SGC-30(a), CGC-30(b), SGC-60(c) and CGC-60(d).

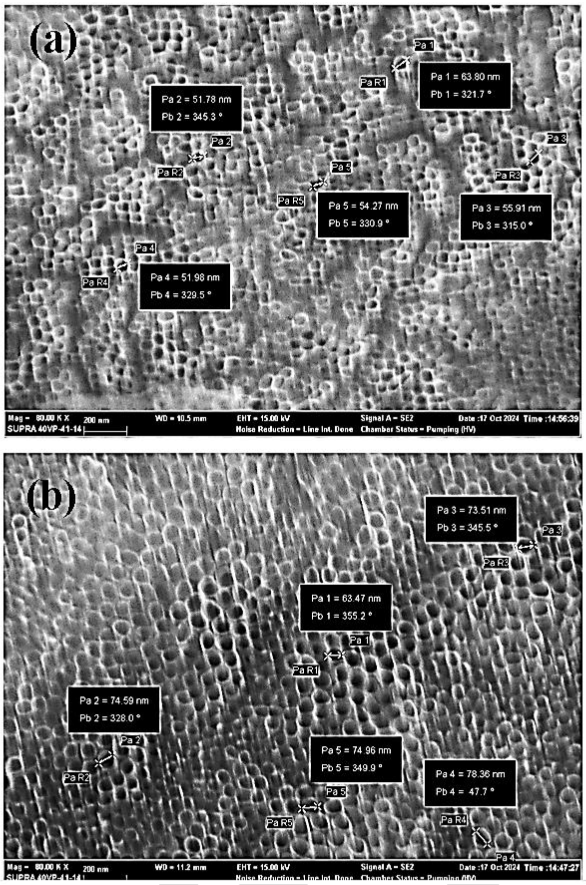

Figure 3. FE-SEM images of SGC-30 (a) and SGC-60 (b).

Figure 4 (a-d) shows the contact angle images of samples after the anodic oxidation process. As seen in Figures 4 (a-c-d), the contact angle values of the SGC-30, SGC-60 and CGC-60 samples were determined to be 100.93°, 99.27° and 100.98°, respectively. These similar contact angle values did not show a significant change over time when the square cathode was used. As a result of 60 minutes of anodic oxidation process with cylinder cathode, the contact angle of the surface gave similar results with square cathode applications. But in Figure 4 (b), the contact angle value of the CGC-30 sample was determined to be 81.17°, which is the lowest value compared to the others. From these results, it was concluded that time was an effective parameter for the contact angles regardless of the cathode type. The contact angle value for Ti6Al4V alloy reported in the literature is 61.7°-61.1°, respectively (Hamil et al., 2022; Yu et al., 2015). In this study, it was determined that the surfaces of samples, except for CGC-30, became hydrophobic (contact angle > 90°) as the high contact angle values. It has been reported in the literature that Ti6Al4V surfaces exhibit hydrophilic properties, while nanotube-coated surfaces exhibit hydrophobic properties. Additionally, it is known that the hydrophobic/hydrophilic behaviour of a surface depends on factors such as surface load, surface energy, surface roughness, and surface porosity (Durdu et al., 2021). Surface roughness analysis was also performed to better understand the contact angle results of this study. Surface roughness profile images and R values were shown in Figure 5 (a-d). As shown in Figure 5 (a-b-d), the surface roughness Ra values were determined to be 0.07µm, 0.06µm, and 0.07µm for the samples labelled SGC-30, CGC-30, and CGC-60, respectively. However, the sample labelled SGC-60 exhibited the highest Ra value of 0.11µm. Gao et al. reported that surface roughness and contact angle values increased with anodic oxidation treatment time on the Ti6Al4V alloy, which is consistent with the results obtained in this study (Gao et al., 2014). Durdu et al. reported that contact angle values generally increased as the nanotube diameters increased, resulting in surfaces exhibiting hydrophobic behaviour (Durdu et al., 2021). In this study, the nanotube diameter was high at 60 minutes of anodic oxidation (Figure 3(a-b)).

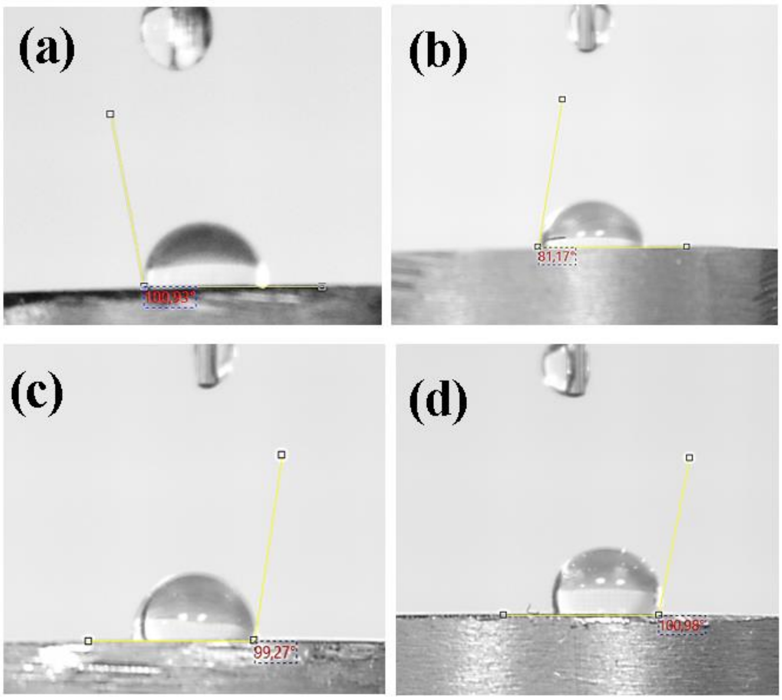

Figure 4. Contact angle images of SGC-30(a), CGC-30(b), SGC-60(c) and CGC-60(d)

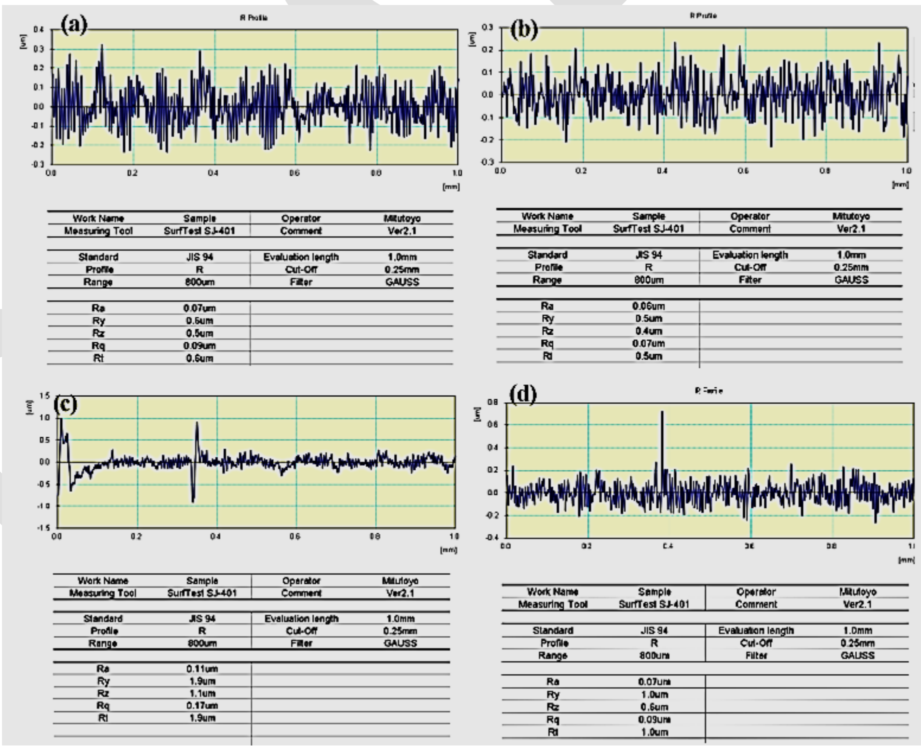

Figure 5. Surface roughness profiles of SGC-30 (a), CGC-30 (b), SGC-60 (c) and CGC-60 (d).

CONCLUSION

In this study, the effect of cathode shape and anodization time on the formation of TiO_2 nanotubes on Ti6Al4V-ELI alloy was investigated. In this study, the anodic oxidation process was carried out using square and cylindrical cathodes for 30 and 60 minutes. 30 minutes and the cylindrical cathode were not sufficient to observe the regular nanotube structure, but the most uniform tube distribution was observed at 60 minutes. Compared to the other samples in the study, the average nanotube diameter of the SGC-60 coded sample, which has the preferred nanotube structure, is 73.02 nm. Except for the CGC-30 sample, all other samples showed a hydrophobic surface with a contact angle greater than 90°. Surface roughness analysis showed similar results, but the sample labelled SGC-60 exhibited the highest Ra value of 0.11µm.

ACKNOWLEDGEMENTS
This work has been supported by TUBITAK- 2210/C National MSc/MA Scholarship Program in the Priority Fields in Science and Technology.

REFERENCES

Andoko, A., Khoyroh, S. B., Aminnudin, A., &Prasetya, R. (2024). Overview of anodization and silver coating for titanium alloys: Process parameters and biomedical insights. Mechanical Engineering for Society and Industry, 4(3), 318-336.

Ansari, Z., Kalantar, M., Kharaziha, M., Ambrosio, L., &Raucci, M. G. (2020). Polycaprolactone/fluoride-substituted hydroxyapatite (PCL/FHA) nanocomposite coatings prepared by in-situ sol–gel process for dental implant applications. Progress in Organic Coatings, 147, 105873.

Durdu, S., Sancak, M., Yalcin, E., Usta, M., Akagunduz, E., &Altinkok, A. (2021). Surface characterization of TiO_2 nanotube arrays produced on Ti–6Al–4V alloy by anodic oxidation. Surface and Coatings Technology, 428, 127903.

Gabor, R., Doubkova, M., Gorosova, S., Malanik, K., Vandrovcova, M., Cvrcek, L., ... &Bacakova, L. (2020). Preparation of highly wettable coatings on Ti–6Al–4V ELI alloy for traumatological implants using micro-arc oxidation in an alkaline electrolyte. Scientific Reports, 10(1), 19780.

Gao, Y., Sun, Y., & Guo, D. (2014). Facile fabrication of superhydrophobic surfaces with low roughness on Ti–6Al–4V substrates via anodization. Applied Surface Science, 314, 754–759.

Gaona-Tiburcio, C., Jáquez-Muñoz, J. M., Nieves-Mendoza, D., Maldonado-Bandala, E., Lara-Banda, M., Lira-Martinez, M. A., ... &Almeraya-Calderon, F. (2024). Corrosion behavior of titanium alloys (Ti CP2, Ti–6Al–2Sn–4Zr–2Mo, Ti–6Al–4V and Ti Beta-C) with anodized and exposed in NaCl and H_2SO_4 solutions. Metals, 14(2), 160.

Gong, D., Grimes, C. A., Varghese, O. K., Hu, W., Singh, R. S., Chen, Z., & Dickey, E. C. (2001). Titanium oxide nanotube arrays prepared by anodic oxidation. Journal of Materials Research, 16, 3331–3334.

Hamil, M. I., Abdulwahid, K. I., & AL-Shakban, M. (2022). Improvement of corrosion and osseointegration characteristics for Ti–6Al–4V alloy by coating with polyetheretherketone (PEEK) and nanohydroxyapatite using electrophoretic deposition for biomedical applications. Journal of Nanostructures, 12(4), 826–841.

Jarosz, M., Pawlik, A., Kapusta-Kołodziej, J., Jaskuła, M., & Sulka, G. D. (2014). Effect of the previous usage of electrolyte on growth of anodic titanium dioxide (ATO) in a glycerol-based electrolyte. Electrochimica Acta, 136, 412–421.

Jáquez-Muñoz, J. M., Gaona-Tiburcio, C., Méndez-Ramírez, C. T., Baltazar-Zamora, M. Á., Estupinán-López, F., Bautista-Margulis, R. G., ... &Almeraya-Calderón, F. (2023). Corrosion of titanium alloys anodized using electrochemical techniques. Metals, 13(3), 476.

Jáquez-Muñoz, J. M., Gaona-Tiburcio, C., Mendez-Ramirez, C. T., Carrera-Ramirez, M. G., Baltazar-Zamora, M. A., Santiago-Hurtado, G., ... &Almeraya-Calderon, F. (2024). Corrosion of anodized titanium alloys. Coatings, 14(7), 809.

Kapusta-Kołodziej, J., Syrek, K., Pawlik, A., Jarosz, M., Tynkevych, O., & Sulka, G. D. (2017). Effects of anodizing potential and temperature on the growth of anodic TiO_2 and its photoelectrochemical properties. Applied Surface Science, 396, 1119–1129.

Kapusta-Kołodziej, J., Tynkevych, O., Pawlik, A., Jarosz, M., Mech, J., & Sulka, G. D. (2014). Electrochemical growth of porous titanium dioxide in a glycerol-based electrolyte at different temperatures. Electrochimica Acta, 144, 127–135.

Kiel, M., Szewczenko, J., Marciniak, J., &Nowińska, K. (2012). Electrochemical properties of Ti–6Al–4V ELI alloy after anodization. In Information Technologies in Biomedicine: Third International Conference, ITIB 2012, Gliwice, Poland, June 11–13, 2012. Proceedings (pp. 369–378). Springer Berlin Heidelberg.

Kim, J. H., Zhu, K., Kim, J. Y., & Frank, A. J. (2013). Tailoring oriented TiO_2 nanotube morphology for improved Li storage kinetics. Electrochimica Acta, 88, 123–128.

Lario, J., Viera, M., Vicente, A., Igual, A., & Amigo, V. (2019). Corrosion behaviour of Ti–6Al–4V ELI nanotubes for biomedical applications. Journal of Materials Research and Technology, 8(6), 5548–5556.

Matykina, E., Hernandez-López, J. M., Conde, A., Domingo, C., De Damborenea, J. J., & Arenas, M. A. (2011). Morphologies of nanostructured TiO_2 doped with F on Ti–6Al–4V alloy. Electrochimica Acta, 56(5), 2221–2229.

Mazierski, P., Nischk, M., Gołkowska, M., Lisowski, W., Gazda, M., Winiarski, M. J., ... &Zaleska-Medynska, A. (2016). Photocatalytic activity of nitrogen-doped TiO_2 nanotubes prepared by anodic oxidation: The effect of applied voltage, anodization time and amount of nitrogen dopant. Applied Catalysis B: Environmental, 196, 77–88.

Wang, L. N., Jin, M., Zheng, Y., Guan, Y., Lu, X., & Luo, J. L. (2014). Nanotubular surface modification of metallic implants via electrochemical anodization technique. International Journal of Nanomedicine, 4421–4435.

Yavari, S. A., Chai, Y. C., Böttger, A. J., Wauthle, R., Schrooten, J., Weinans, H., &Zadpoor, A. A. (2015). Effects of anodizing parameters and heat treatment on nanotopographical features, bioactivity, and cell culture response of additively manufactured porous titanium. Materials Science and Engineering: C, 51, 132–138.

Yu, X., Tan, L., Yang, H., & Yang, K. (2015). Surface characterization and preparation of Ta coating on Ti–6Al–4V alloy. Journal of Alloys and Compounds, 644, 698–703.